

Solution and Solid-State Structures of Phosphine Adducts of Monomeric Zinc Bisphenoxide Complexes. Importance of These Derivatives in CO₂/Epoxide Copolymerization Processes[†]

Donald J. Darensbourg,* Marc S. Zimmer, Patrick Rainey, and David L. Larkins

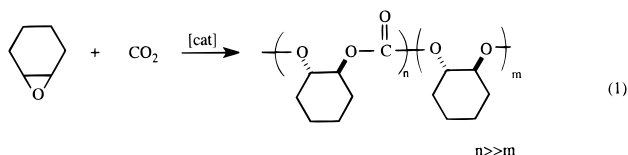
Department of Chemistry, Texas A&M University, P.O. Box 30012, College Station, Texas 77842-3012

Received May 24, 1999

Phosphine derivatives of the monomeric zinc phenoxide complexes, (phenoxide)₂ZnL_n, where phenoxide equals 2,6-di-*tert*-butylphenoxide, 2,4,6-tri-*tert*-butylphenoxide, and 2,6-diphenylphenoxide and *n* = 1 or 2, have been synthesized from the reaction of Zn[N(SiMe₃)₂]₂ and the corresponding phenol followed by the addition of phosphine. The complexes have been characterized in solution by ³¹P NMR spectroscopy and in selected instances in the solid-state by X-ray crystallography. The small, basic phosphine, PMe₃, provided the only case of an isolated complex possessing two phosphine ligands (i.e., *n* = 2). For all other larger phosphines only the monophosphine adducts were obtained. Furthermore, only fairly basic phosphines were found to bind to zinc, e.g., whereas PPh₃ (p*K*_a = 2.73) was ineffective, PPh₂Me (p*K*_a = 4.57) did form a strong bond to zinc. The solid-state structures of the monophosphine adducts consist of a near-trigonal planar geometry about the zinc center, where the average P–Zn–O angles are larger than the O–Zn–O angles. On the other hand, the bisphosphine adduct, Zn(O-2,4,6-*t*-Bu₃C₆H₂)₂·2PMe₃, is a distorted tetrahedral structure with O–Zn–O and P–Zn–P bond angles of 108.8(2)° and 107.1(9)°, respectively. Competitive phosphine binding studies monitored by ³¹P NMR spectroscopy provided a relative binding order of PPh₃ ≈ P^{*i*}Bu₃ < PPh₂Me < PCy₃ < PMe₂Ph < PnBu₃ < PEt₃ < PMe₃. Hence, the relative binding of basic phosphine ligands at these congested zinc sites is largely determined by their steric requirements. All phosphine adducts, with the exception of PMe₂Ph and PMe₃, were found to undergo slow self-exchange (<600 s^{–1}) with free phosphine by ³¹P NMR spectroscopy. However, the two small phosphines, PMe₂Ph (cone angle = 122°) and PMe₃ (cone angle = 118°), were shown to undergo rapid exchange presumably via an associative mechanism. Although there was no kinetic preferences for PCy₃ binding to cadmium vs zinc, cadmium was thermodynamically favored by about a factor of 2.5. The addition of up to 3 equiv of PCy₃ to the Zn(O-2,4,6-*t*-Bu₃C₆H₂)₂ or Zn(O-2,4,6-*t*-Bu₃C₆H₂)₂ derivatives did not significantly alter the reactivity of these catalysts for the copolymerization of cyclohexene oxide (CHO) and CO₂ to high-molecular weight poly(cyclohexene carbonate). However, the presence of PCy₃ greatly retarded their ability to homopolymerize CHO to polyether or to afford polyether linkages during the copolymerization of CHO/CO₂.

Introduction

A focus of our current research interest is the coupling of CO₂ and epoxides to produce polycarbonates catalyzed via zinc complexes such as (2,6-diphenylphenoxide)₂Zn(THF)₂.^{1,2} Other closely related contributions to this area involving isolated zinc complexes have recently been reported.^{3–5} Specifically, the process depicted in eq 1 is under investigation because copolymerization is highly favored over cyclic carbonate production in this instance. Nevertheless, polyether formation still occurs and remains a process we wish to minimize in all CO₂/epoxide copolymerization reactions.



[†] Dedicated to Professor Heinrich Vahrenkamp on the occasion of his 60th birthday.

- (1) Darensbourg, D. J.; Holtcamp, M. W. *Macromolecules* **1995**, *28*, 7577.
- (2) Darensbourg, D. J.; Holtcamp, M. W.; Struck, G. E.; Zimmer, M. S.; Niezgoda, S. A.; Rainey, P.; Robertson, J. B.; Draper, J. D.; Reibenspies, J. H. *J. Am. Chem. Soc.* **1999**, *121*, 107.
- (3) Super, M.; Berluche, E.; Costello, C.; Beckman, E. *Macromolecules* **1997**, *30*, 368.

Because the copolymerization process appears to proceed via an anionic coordinative mechanism, it is of interest to examine the binding of various donor ligands at the active metal site.⁶ Organophosphines have long been exploited in homogeneous catalysis as ancillary ligands because of the ability to systematically vary the substituents on the phosphorus and, hence, the steric and electronic properties of the phosphine.^{7–14} In addition, we wish to assess the influence of phosphine ligands on the reactivity of the metal center with regard to the CO₂/epoxide coupling reaction depicted in eq 1. Relevant to these studies,

- (4) Super, M.; Beckman, E. J. *Macromol. Symp.* **1998**, *127*, 89.
- (5) Cheng, M.; Lobkovsky, E. B.; Coates, G. W. *J. Am. Chem. Soc.* **1998**, *120*, 11018.
- (6) Darensbourg, D. J.; Niezgoda, S. A.; Holtcamp, M. W.; Draper, J. D.; Reibenspies, J. H. *Inorg. Chem.* **1997**, *36*, 2426.
- (7) Tolman, C. A. *Chem. Rev.* **1977**, *77*, 313.
- (8) Rahman, Md. M.; Liu, H. Y.; Prock, A.; Giering, W. P. *Organometallics* **1987**, *6*, 650.
- (9) Brown, T. L. *Inorg. Chem.* **1992**, *31*, 1286.
- (10) Grubbs, R. H.; Nguyen, S. T.; Ziller, J. W. *J. Am. Chem. Soc.* **1993**, *115*, 9858.
- (11) Cole Hamilton, D. J.; MacDougall, J. K.; Simpson, M. C.; Green, M. J. *J. Chem. Soc., Dalton Trans.* **1996**, 1161.
- (12) Casey, C. P.; Paulsen, E. L.; Beuttenmeuller, E. W.; Proft, B. R.; Petrovich, L. M.; Matler, B. A.; Powell, D. R. *J. Am. Chem. Soc.* **1997**, *119*, 11817.
- (13) Osborn, J. A.; Schrock, R. R. *J. Am. Chem. Soc.* **1976**, *98*, 2134.
- (14) Farnetti, E.; Kaspar, J.; Spogliarish, R.; Gragiani, M. *J. Chem. Soc., Dalton Trans.* **1988**, 947.

phosphine derivatives of zinc are rather rare with most investigations focusing on ^{31}P NMR studies of phosphine derivatives of zinc halides.^{15,16} Crystallographically characterized examples are limited to the chemical vapor deposition (CVD) candidates $\text{Zn}(\text{S}-2,4,6\text{-t-Bu}_3\text{C}_6\text{H}_3)_2(\text{Ph}_2\text{PMe})$,¹⁷ $(\text{Et}_2\text{NCS}_2)_2\text{Zn}(\text{PMe}_3)$,¹⁸ and the zinc halide structure $[\text{ZnI}_2(\text{PEt}_3)]_2$.¹⁹ Herein, we present the synthesis, solid-state, and solution structures of phosphine adducts of active catalysts for the copolymerization of cyclohexene oxide and CO_2 , (bisphenoxide)zinc complexes.²⁰

Experimental Section

Methods and Materials. All syntheses and manipulations were carried out on a modified Schlenk line or in a glovebox under argon. Glassware was flamed out thoroughly before use. Toluene, hexane, and benzene were freshly distilled from sodium benzophenone, and dichloromethane was distilled from P_2O_5 prior to their use. Diphenylmethylphosphine and bisdicyclohexylphosphinomethane were purchased from Strem and stored in a glovebox. Trimethylphosphine was purchased from Aldrich and stored in a Schlenk tube under an atmosphere of argon. Triethylphosphine and tricyclohexylphosphine were purchased from Aldrich and were stored in a glovebox. Tri-*n*-butylphosphine (>90% purity) was purchased from Aldrich packaged as a sure-seal container and was stored under argon atmosphere. All phosphines were used without further purification. The phenols 2,6-di-*tert*-butylphenol, 2,6-diphenylphenol, 2,4,6-trimethylphenol, and 2,4,6-tri-*tert*-butylphenol were all purchased from Aldrich. The 2,4,6-tri-*tert*-butylphenol is very hygroscopic and was purified by means of sublimation in vacuo before use (bath temperature ca. 100 °C, 3.5 mmHg). $\text{Zn}[\text{N}(\text{SiMe}_3)_2]_2$ was prepared according to the published procedure and isolated through distillation in vacuo as a clear, slightly viscous liquid (bp = 103–104 °C, 4 mmHg).¹⁶ This material is extremely moisture-sensitive and, as such, was stored in a glovebox and used immediately after removal from the box. ^{31}P NMR data were acquired on Varian XL200 and Unity+ 300 MHz superconducting NMR spectrometers operating at 81 and 121 MHz, respectively. Both instruments are equipped with variable-temperature control modules. All ^{31}P NMR data are referenced to H_3PO_4 (85% in D_2O). ^1H and ^{13}C NMR spectra were acquired on Varian XL200E, Unity+ 300 MHz, and VXR 300 MHz superconducting NMR spectrometers. The operating frequencies for ^{13}C experiments were 50.29 and 75.41 MHz for the 200 and 300 MHz instruments, respectively. Infrared spectra were recorded on a Mattson 6021 FT-IR spectrometer with DTGS and MCT detectors.

Synthesis of $\text{Zn}(\text{O}-2,6\text{-t-Bu}_2\text{C}_6\text{H}_3)_2(\text{PPh}_2\text{Me})$ (1). To $\text{Zn}[\text{N}(\text{SiMe}_3)_2]_2$ (0.195 g, 0.5 mmol) in 5 mL of toluene was added a 5 mL toluene solution of 2,6-di-*tert*-butylphenol (0.206 g, 1 mmol). The mixture was stirred for 15 min followed by the addition of PPh_2Me (0.10 g, 0.5 mmol) via a syringe. Stirring of the reaction solution was continued for an additional 30 min, and then the solution was concentrated in vacuo to approximately 2–3 mL. Crystals were obtained through slow diffusion of hexane into the toluene reaction at –20 °C over several days. The yield after drying was 0.16 g (48%). Anal. Calcd for $\text{ZnC}_{41}\text{H}_{55}\text{O}_2\text{P}$: C, 71.1; H, 8.15. Found: C, 72.85; H, 8.14. ^1H NMR (CD_2Cl_2): δ 1.25 (d, $J_{\text{P-H}} = 6.8$ Hz, 3H, PCH_3), 1.61 (s, 18H, $\text{C}(\text{CH}_3)_3$), 6.8–7.2 (m, 16H, Ph), 7.38 (d, 2H, *p*- C_6H_3). ^{13}C NMR (CD_2Cl_2): δ 31.92 ($\text{C}(\text{CH}_3)_3$), 35.93 (PCH_3), 165.64 (*ipso*- C_6H_3). ^{31}P NMR (CD_2Cl_2): δ –19.9.

Syntheses of the other monophosphine derivatives of $\text{Zn}(\text{O}-2,6\text{-t-Bu}_2\text{C}_6\text{H}_3)_2$ were accomplished in a manner analogous to that described for complex 1.

$\text{Zn}(\text{O}-2,6\text{-t-Bu}_2\text{C}_6\text{H}_3)_2(\text{PCy}_3)$ (2). Crystals of **2** were grown from the concentrated toluene solution overnight at 0 °C, providing 0.19 g (54%) of the product. Anal. Calcd for $\text{ZnC}_{46}\text{H}_{75}\text{O}_2\text{P}$: C, 72.6; H, 9.88. Found: C, 73.1; H, 9.90. ^1H NMR (C_6D_6): δ 0.8–2 (m, 33H, $\text{PCy}_3\text{H}_{11}$), 1.77 (s, 18H, CCH_3), 6.81 (t, 2H, *p*- C_6H_3). ^{13}C NMR (C_6D_6): δ 27.6–32 ($\text{PCy}_3\text{H}_{11}$), 32.5, 165.2 (*ipso* C_6H_3). ^{31}P NMR (C_6D_6): δ 7.74.

$\text{Zn}(\text{O}-2,6\text{-t-Bu}_2\text{C}_6\text{H}_3)_2(\text{PMe}_3)$ (3). After the volatiles were removed under vacuum, the material was washed twice with cold hexanes, resulting in a white powdery solid in 47% isolated yield. ^1H NMR: δ 0.252 (d, $J_{\text{P-H}} = 8.7$ Hz, PCH_3), 1.66 (s, 18H, CCH_3), 6.81 (t, 2H, *p*- C_6H_3), 7.33 (d, 4H, *m*- C_6H_3). ^{13}C NMR (C_6D_6): δ 10.95 (d, $J_{\text{P-C}} = 24.2$ Hz), 30.36 (CCCH_3), 31.77 (CCH_3), 115.89, 125.29, 138.82, 165.33 (*ipso*- C_6H_3). ^{31}P NMR (C_6D_6): δ –48.9.

$\text{Zn}(\text{O}-2,6\text{-t-Bu}_2\text{C}_6\text{H}_3)_2(\text{PET}_3)$ (4). A microcrystalline material grew from a toluene solution that had been concentrated down to about 2 mL. The final yield after drying was 0.11 g (37%). ^1H NMR (C_6D_6): δ 0.98 (m, 9H, PCH_2CH_3), 1.22 (m, 6H, PCH_2CH_3), 6.92 (t, 2H, *p*- C_6H_3), 7.37 (d, 4H, *m*- C_6H_3). ^{31}P NMR (C_6D_6): δ –14.0.

$\text{Zn}(\text{O}-2,6\text{-t-Bu}_2\text{C}_6\text{H}_3)_2(\text{PBu}_3)$ (5). A white powdery solid (0.137 g, 81% yield) was left behind after the material was washed twice in cold hexanes. ^1H NMR (C_6D_6): δ 0.67–1.23 (m, 9H, PBu), 1.72 (s, 18H, CCH_3), 6.803 (t, 2H, *p*- C_6H_3), 7.33 (d, 4H, *m*- C_6H_3). ^{13}C NMR (C_6D_6): δ 13.42, 20.64 (d, PCH_2), 24.34, 24.52, 115.74, 125.09, 138.70, 165.09 (*ipso*- C_6H_3). ^{31}P NMR (C_6D_6): δ –21.0.

Synthesis of $[\text{Zn}(\text{O}-2,6\text{-t-Bu}_2\text{C}_6\text{H}_3)_2]_2(\text{PCy}_2)_2\text{CH}_2$ (6). Bisdicyclohexylphosphinomethane (0.1 g, 0.00025 mol) and 2,6-di-*tert*-butylphenol (0.206 g, 0.0005 mol) were dissolved in 5 mL of toluene. The toluene solution was then added to neat $\text{Zn}[\text{N}(\text{SiMe}_3)_2]_2$ and was stirred for 0.5 h. The volatiles were then stripped away in vacuo, giving a slightly yellowed fine powder in 82% yield. ^{31}P NMR (C_6D_6): δ –3.77.

$[\text{Zn}(\text{O}-2,6\text{-t-Bu}_2\text{C}_6\text{H}_3)_2]_2(\text{Me}_2\text{PPh})$ (7). After the volatiles were removed under vacuum, the product was washed several times with cold hexanes to provide a white powdery solid in 52% yield. ^1H NMR (C_6H_6): δ 0.72 (d, PCH_3), 1.64 (s, 18H, CCH_3), 6.89 (t, 2H, *p*- C_6H_3), 7.37 (d, 4H, *m*- C_6H_3). ^{31}P NMR (C_6H_6): δ –35.8.

Synthesis of $\text{Zn}(\text{O}-2,4,6\text{-t-Bu}_3\text{C}_6\text{H}_3)_2(\text{PMe}_3)_2$ (8). A 5 mL toluene solution of 2,4,6-tri-*tert*-butylphenol (0.33 g, 1.3 mmol) was added to $\text{Zn}[\text{N}(\text{SiMe}_3)_2]_2$ (0.25 g, 0.65 mmol) dissolved in 3 mL of toluene. After the solution was stirred for 30 min, 1 equiv of trimethylphosphine (0.134 μL , 0.65 mmol) was added via a syringe. The mixture was stirred for an extra 15 min and then concentrated down to 1–2 mL. A second equivalent of the phosphine was then added. Very large block crystals of the product grew from the solution overnight at –20 °C. The overall yield was 0.96 g (20%).

Synthesis of $\text{Zn}(\text{O}-2,6\text{-Ph}_2\text{C}_6\text{H}_3)_2(\text{Ph}_2\text{PMe})$ (9). 2,6-Diphenylphenol (0.12 g, 1 mmol) in 5 mL of toluene was added to $\text{Zn}[\text{N}(\text{SiMe}_3)_2]_2$ (0.195 g, 0.5 mmol) dissolved in 3 mL of toluene. The mixture was stirred for 30 min followed by addition of Ph_2PMe . After the mixture was stirred for an additional 30 min, the volatiles were pulled away in vacuo, leaving behind a tacky, foamy solid. The material was stirred in cold hexane and filtered, giving 0.28 g (73%) of the white powdery product. ^1H NMR (CD_2Cl_2): δ 3.24 (d, 3H), 6.4–7.4 (m, 36H, phenyl). ^{13}C NMR (CD_2Cl_2): δ 55.2 (PCH_3), 115.3, 121.1, 126, 128.2, 128.5, 128.9, 129.1, 129.3, 132.1, 138, 141.9. ^{31}P NMR (CD_2Cl_2): δ 0.29.

Synthesis of $\text{Zn}(\text{O}-2,6\text{-Ph}_2\text{C}_6\text{H}_3)_2(\text{PCy}_3)$ (10). Preparation and isolation were very similar to that for **9**. Removal of the toluene in vacuo left a colorless oil. Pentane was added to the oil, and after the mixture was stirred for several minutes, the product was isolated as a white powder in 48% yield. ^1H NMR (C_6D_6): δ 0.8–1.6 (b, 33H, $\text{PCy}_3\text{H}_{11}$), 6.58 (t, 2H, *p*- C_6H_3), 6.85–7.5 (b, 22H, Ph). ^{13}C NMR (C_6D_6): δ 26.1, 27.3 (d), 29.3, 30.5 (d), 116, 123.2, 142, 160.5 (*ipso*). ^{31}P NMR (C_6D_6): δ 12.2.

Synthesis of $\text{Zn}(\text{O}-2,6\text{-Ph}_2\text{C}_6\text{H}_3)_2(\text{PMe}_3)$ (11). Complex **11** was made in a fashion analogous to that of **9** and isolated as a solid in 57% yield. ^1H NMR (C_6D_6): δ –0.49 (d, 9H, $J_{\text{P-H}} = 14.1$), 6–7.35 (m, 14H), 7.812 (d, 4H, *m*- C_6H_3). ^{31}P NMR (C_6D_6): δ –47.4.

Synthesis of $\text{Zn}(\text{O}-2,6\text{-Ph}_2\text{C}_6\text{H}_3)_2(\text{PET}_3)$ (12). The synthesis was similar to that for **9** and isolated in 32% yield. ^1H NMR (C_6D_6): δ 0.42 (m, 3H, PCH_2CH_3), 0.63 (m, 2H, PCH_2CH_3), 6.87 (t, 2H), 7.39 (d, 4H, *o*- C_6H_3), 7.86 (d, 4H, *m*- C_6H_3). ^{31}P NMR (C_6D_6): δ –12.1 (b).

- (15) Goel, R. G.; Henry, W. P.; Jha, N. K. *Inorg. Chem.* **1982**, *21*, 2551.
- (16) Goel, R. G.; Ogiini, W. O. *Inorg. Chem.* **1977**, *16*, 1968.
- (17) Bochmann, M.; Bwembya, G. C.; Grinter, R.; Powell, A. K.; Webb, K.; Hursthouse, M. B.; Abdul-Malik, K. M.; Magid, M. A. *Inorg. Chem.* **1994**, *33*, 2290.
- (18) Zeng, D.; Hampden-Smith, M. J.; Alam, T. M.; Rheingold, A. L. *Polyhedron* **1994**, *13*, 2715.
- (19) McAuliffe, C. A.; Bricklebank, N.; Godfrey, S. M.; Mackie, A. G.; Pritchard, R. G. *J. Chem. Soc., Chem. Commun.* **1992**, 944.
- (20) Darensbourg, D. J.; Zimmer, M. S.; Rainey, P.; Larkins, D. L. *Inorg. Chem.* **1998**, *37*, 2852.

Table 1. Crystallographic Data and Data Collection Parameters for Complex **8**

formula	C ₄₂ H ₇₆ O ₂ P ₂ Zn
fw	740.34
cryst system	monoclinic
space group	P2 ₁ /c
<i>a</i> , Å	18.271(4)
<i>b</i> , Å	14.648(3)
<i>c</i> , Å	18.930(4)
β , deg	117.06
<i>V</i> , Å ³	4511.9(16)
<i>Z</i>	4
<i>d</i> (calcd), g/cm ³	1.090
abs coeff, mm ⁻¹	1.639
goodness of fit ^a on <i>F</i> ²	1.069
λ , Å	1.541 84
<i>T</i> , K	193(2)
<i>R</i> , ^b %	6.83
<i>R</i> _w , ^c %	14.53

^a GOF = $[\sum(w(F_o^2 - F_c^2)^2)/(n - p)]^{1/2}$, where *n* = no. of data and *p* = no. of parameters. ^b *R* = $\sum(|F_o| - |F_c|)/\sum F_o$. ^c *R*_w = $\{[\sum w(F_o^2 - F_c^2)^2]/[\sum w(F_o^2)^2]\}^{1/2}$.

Synthesis of Zn(O-2,6-Ph₂C₆H₃)₂(PBu₃) (13). Complex **13** was made in a fashion analogous to that of **9** and isolated in 22% yield. The product was a sticky colorless solid. ¹H NMR (C₇D₈): δ 0.74 (m, 7H, PCH₂CH₃), 1.30 (p, 2H, PCH₂), 6.7–7.5 (m, 22H, Ph), 7.83 (b, 4H, *m*-C₆H₃). ³¹P NMR (C₇D₈): δ -18.6 (b).

Synthesis of Zn(O-2,4,6-trimethyl-C₆H₂)₂(PMe₃)₂ (14). To Zn-[N(SiMe₃)₂]₂ (0.095 g, 0.25 mmol) in 5 mL of toluene was added 2,4,6-trimethylphenol (0.068 g, 0.5 mmol) as a toluene solution dropwise over the course of several minutes. After approximately 20% of the phenol had been added, a white solid began to precipitate. The remaining phenol was added and the mixture stirred for an additional 30 min. PMe₃ (0.052 mL, 0.5 mmol) was then added via a syringe. The solution cleared almost instantaneously as a reaction took place. The mixture was then stirred for 10 more minutes. While the toluene was removed in vacuo, the PMe₃ was also evacuated and the material reprecipitated and could not be redissolved in any common solvent.

Synthesis of Zn(O-2,4,6-trimethyl-C₆H₂)₂(PBu₃)₂ (15). Complex **15** was made in a manner similar to that used for **14**. Removal of the toluene left a moist white solid that did not appear to dry further when left under vacuum for an extended period of time. ³¹P NMR (C₆D₆): δ -31.5 (free PBu₃), -21.0 (bound PBu₃), 63.0 (bound PBu₃O)).

Phosphine Competition Studies. A sample of pure Zn(O-2,6-^{*t*}Bu₂C₆H₃)₂(PCy₃), crystallized from a concentrated toluene solution, was dissolved in CD₂Cl₂ and added to an NMR tube in a glovebox. An equimolar amount of the appropriate phosphine was added via a syringe with vigorous shaking to ensure complete dissolution of the phosphine. ³¹P NMR data were recorded at -80, -60, -40, -20, 0, and 20 °C. Ordering of the phosphine affinities was established on the basis of the amount of PCy₃ displaced from zinc.

Zinc/Cadmium Competition Study. The synthesis and isolation of Zn(O-2,6-^{*t*}Bu₂C₆H₃)₂(THF)₂ and its cadmium analogue were carried out as described earlier. To a solution of CD₂Cl₂ was added a pure sample of Cd(O-2,6-^{*t*}Bu₂C₆H₃)₂(THF)₂ (0.019 mmol) and an equimolar amount of pure Zn(O-2,6-^{*t*}Bu₂C₆H₃)₂(THF)₂. The contents were placed in an NMR tube and cooled to -78 °C. To a separate tube was added 0.019 mmol of PCy₃ in a 1 mL solution of CD₂Cl₂. This solution was also cooled to -78 °C. After several minutes at -78 °C, the metal complex mixture was cannulated into the phosphine-containing tube. The entire mixture was maintained at -78 °C and then warmed slowly as ³¹P NMR data were acquired at 20 °C temperature increments.

NOTE! Cadmium and its complexes are extremely toxic and should be handled with caution. Cadmium waste products should be stored in a separate, clearly marked container.

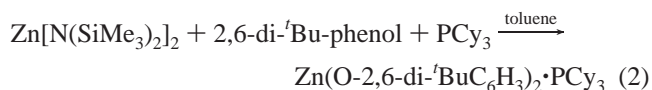
X-ray Crystallography. Crystal data and details of the data collections are provided in Table 1. A colorless block crystal of **8** was mounted on a glass fiber with epoxy cement at room temperature and cooled to 163 K (**8**) in a N₂ stream. Preliminary examination and data

collection were performed on a Rigaku AFC5 X-ray diffractometer (Cu K α , λ = 1.541 78 Å radiation). Cell parameters were calculated from the least-squares fitting of the setting angles for 25 reflections. ω scans for several intense reflections indicated acceptable crystal quality. Data were collected for $8.0^\circ \leq 2\theta \leq 120^\circ$. Three control reflections collected for every 97 reflections showed no significant trends. Lorentz and polarization corrections were applied as was a semiempirical absorption correction to each. Structures were solved by direct methods [SHELXS, SHELXTL-PLUS program package, Sheldrick (1993)]. Full-matrix least-squares anisotropic refinement for all non-hydrogen atoms yielded *R*, *R*_w(*F*²), and *S* values at convergence. Hydrogen atoms were placed at idealized positions with isotropic thermal parameters fixed at 0.08. Neutral atom scattering factors and anomalous scattering correction terms were taken from the International Tables for X-ray Crystallography.

Copolymerizations Reactions. Polymerization experiments were carried out in a Parr 300 mL autoclave high-pressure reactor equipped with a magnetic stirring unit. Prior to reaction, the autoclave was heated to 80 °C in vacuo overnight to remove trace moisture. An appropriate amount of the catalyst (calculated to 0.013 g of Zn content) was then dissolved in the monomers cyclohexene oxide or propylene oxide. The epoxide solution was introduced into the reactor via an injection port, and the reactor was charged to 800 psi of CO₂ and heated to 80 °C for 60–70 h. Methylene chloride was used to extract the sticky, viscous product from the reactor. The polymer was then precipitated from a large volume of methanol and dried in a vacuum oven.

Results and Discussion

Syntheses. The phosphine adducts of the bisphenoxide derivatives of zinc were all synthesized in an analogous manner. That is, 2 equiv of a di- or trisubstituted phenol was added to a pure sample of (bistrimethylsilylamide)zinc in a small volume of toluene under argon, and the reaction solution was stirred at ambient temperature for several minutes. An amount of 1 or 2 equiv of the appropriate phosphine was then added directly to the in situ prepared bisphenoxide zinc derivative. Alternatively, in the case of solid phosphines such as PCy₃, the phenol and the phosphine could be added concurrently (as depicted in eq 2) without any changes in the product distribution. Indeed, the phosphine ligands do not appear to interact with the zinc amide starting complex except at low temperature. All of the products were colorless, and any solution color change to pale-yellow or, further, to light-green was indicative of progressive stages of decomposition. Crystallization from a concentrated toluene solution, when possible, proved to be the best method for isolation of the pure product. Purity was assessed by ¹H and ³¹P NMR spectroscopies and in selected instances via elemental analyses. With the exception of the small phosphine ligand, PMe₃, all the derivatives isolated were monoadducts of the bis-(phenoxide)zinc complexes.



Sterically encumbering substituents in the **2** and **6** positions of the aryl ring of the phenoxide ligands bound to zinc have the effect of solubilizing these bisphenoxide derivatives in the absence of phosphines in a variety of media, including hexane, benzene, and methylene chloride. This is a consequence of the bulky phenoxide groups' ability to hinder extensive aggregation through the oxygen lone pairs. On the other hand, complexes derived from 2,4,6-trimethylphenol are insoluble in most common organic solvents because the methyl groups are not sufficiently bulky to avert phenoxide bridging. Indeed, a DFT study of Zn(O-2,6-Me₂C₆H₃)₂ at the B3LYP level of theory has revealed that the complex is stabilized by 48.5 kcal/mol upon

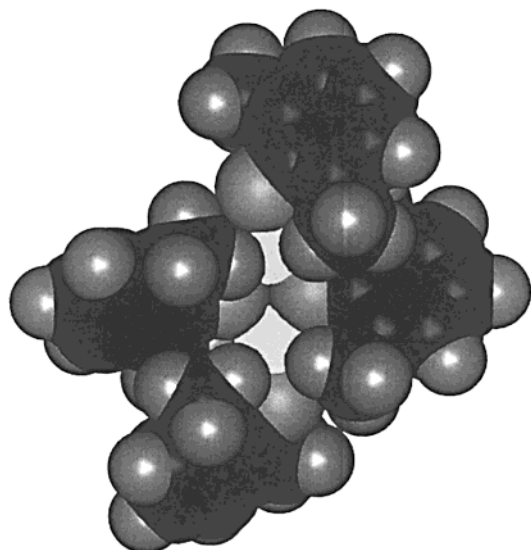


Figure 1. Space-filling model of the optimized dimeric structure of $\{\text{Zn}(\text{O}-2,6\text{-Me}_2\text{C}_6\text{H}_3)_2\}_2$.

forming the phenoxide-bridged dimer.²¹ It has been demonstrated that pyridine is sufficiently basic to disrupt these bridging interactions, and crystals of the complex $\text{Zn}(\text{O}-2,4,6\text{-Me}_3\text{C}_6\text{H}_2)_2(\text{py})_2$ have been obtained from a concentrated solution containing a 1:2 mole ratio of zinc phenoxide to pyridine.² It has recently come to our attention that the bis-2,6-*t*-Bu₂-phenoxide zinc derivative crystallizes from hexane as a dimer that has been characterized in the solid-state by X-ray crystallography.²² Earlier, Caulton and co-workers have reported, on the basis of cryoscopic molecular weight and ¹H NMR measurements in benzene, that the 2,4,6-*t*-Bu₃-phenoxide zinc derivative crystallized from hexanes was dimeric.²³

Because of our success at imparting solubility to the $\{\text{Zn}(\text{O}-2,4,6\text{-Me}_3\text{C}_6\text{H}_2)_2\}_2$ upon addition of pyridine, we anticipated that phosphines would likewise disassemble the aggregate species via σ donation to the metal center. The results were mixed, however, because several phosphine ligands, including PPh_2Me and PCy_3 , failed to draw the toluene insoluble complex into solution. By contrast, when 2 equiv of PMe_3 was added to the insoluble dimer, the complex was rapidly solubilized to afford $\text{Zn}(\text{O}-2,4,6\text{-Me}_3\text{C}_6\text{H}_2)_2 \cdot 2\text{PMe}_3$. Hence, the larger phosphines are incapable of penetrating zinc's sterically hindered inner coordination sphere to affect substitution (see Figure 1 for a space-filling model of the optimized dimeric structure of $\{\text{Zn}(\text{O}-2,4\text{-Me}_2\text{C}_6\text{H}_3)_2\}_2$). Attempted removal of toluene in vacuo from a solution of the bistrimethylphosphine adduct resulted in a reprecipitation of the aggregate species, indicating that the highly volatile PMe_3 ligand is easily dissociated. Similarly, the less-volatile phosphine *n*-Bu₃P readily causes the trimethylphenoxide derivative to dissolve in toluene; however, as expected for the less volatile phosphine, the complex remained in solution during the removal of solvent under vacuum.

Description of Structures. Previously, we have communicated the solid-state structures of complexes **1** and **2**, the

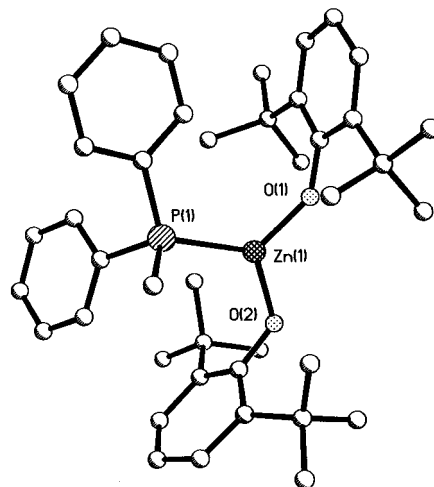


Figure 2. Ball-and-stick drawing of complex **1**.

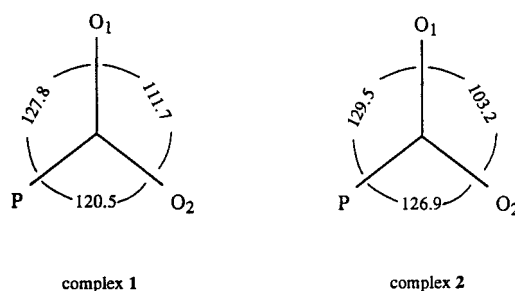


Figure 3. Bond angles in the trigonal planes of complexes **1** and **2**.

mono- PPh_2Me and PCy_3 adducts of $\text{Zn}(\text{O}-2,6\text{-}i\text{-Bu}_2\text{C}_6\text{H}_3)_2$.²⁰ One of these structures, complex **1**, is reproduced in a ball-and-stick drawing in Figure 2. These derivatives have a nearly planar arrangement of the zinc center along with the three atoms in its coordination sphere. That is, the zinc atom lies 0.009(2) and 0.070(2) Å out of the plane defined by the phosphorus and two oxygen donor groups for complexes **1** and **2**, respectively. As depicted in Figure 3, the average $\text{P}-\text{Zn}-\text{O}$ angle is larger than the $\text{O}-\text{Zn}-\text{O}$ angle in both instances. The $\text{Zn}-\text{P}$ bond length in the PPh_2Me derivative at 2.375(2) Å is shorter than that observed in the PCy_3 adduct of 2.433(2) Å. This is somewhat unexpected because PCy_3 is the better donating phosphine. Furthermore, the $\text{O}-\text{Zn}-\text{O}$ angle in the PCy_3 derivative is less obtuse, which would suggest a shorter $\text{Zn}-\text{P}$ bond length in this instance based on hybridization arguments.¹⁷ Evidently, the difference in $\text{Zn}-\text{P}$ bond lengths simply can be traced to the larger steric requirement of the tricyclohexylphosphine ligand.

As previously mentioned, when the phosphine ligand is small, it is possible to observe the binding of a second ligand to the parent $\text{Zn}(\text{O}-2,6\text{-}i\text{-Bu}_2\text{C}_6\text{H}_3)_2$ derivative. For example, upon addition of 2 equiv of PMe_3 to $\text{Zn}(\text{O}-2,4,6\text{-}i\text{-Bu}_2\text{C}_6\text{H}_3)_2$, the bisphosphine adduct was isolated and crystals suitable for X-ray analysis were obtained from toluene at -20°C . It was advantageous to synthesize the tri-*tert*-butyl-substituted derivative in this case because of its generally superior crystallization properties. It is noteworthy that Bochmann and co-workers only isolated the mono- PMe_3 adduct of the thiolate analogue of **8** upon reacting $\{\text{Zn}(\text{S}-2,4,6\text{-}i\text{-Bu}_3\text{C}_6\text{H}_2)_2\}_2$ with 8 equiv of PMe_3 in hydrocarbon solvent.¹⁷ A thermal ellipsoid drawing of $\text{Zn}(\text{O}-2,4,6\text{-}i\text{-Bu}_3\text{C}_6\text{H}_2)_2 \cdot 2\text{PMe}_3$, complex **8**, is exhibited in Figure 4. Selected bond lengths and bond angles are provided in Table 2. Comparison of the structural parameters for **8** with those of the copolymerization catalyst, $\text{Zn}(\text{O}-2,6\text{-}i\text{-Bu}_2\text{C}_6\text{H}_3)_2(\text{THF})_2$, illustrates the relatively larger steric demands and better donating

(21) Computations were carried out by Dr. Agnes Derecskei-Kovacs in the Laboratory for Molecular Simulations in the Department of Chemistry at Texas A&M University. Detailed results from this study, which includes a variety of alkoxide and aryloxide zinc derivatives, will be published elsewhere.

(22) Kunert, M.; Klobes, O.; Bräuer, M.; Görls, H.; Anders, E.; Dinjus, E. Proceedings of the 1999 SFB Congress, Jena, Germany, p PA2.

(23) Geerts, R. L.; Huffman, J. C.; Caulton, K. G. *Inorg. Chem.* **1986**, *25*, 1803.

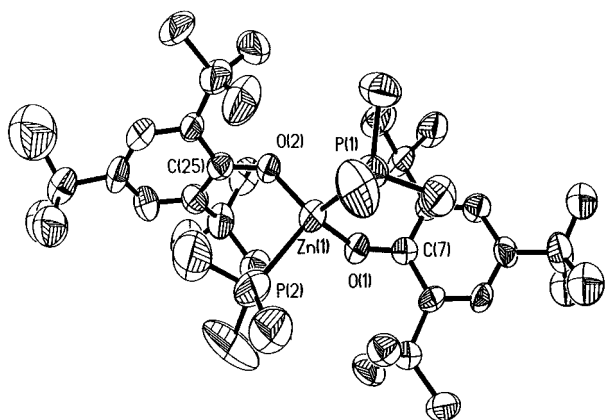


Figure 4. Thermal ellipsoid representation of $\text{Zn}(\text{O}-2,4,6\text{-Bu}_3\text{C}_6\text{H}_2)_2 \cdot 2\text{PMe}_3$, complex **8**.

Table 2. Selected Bond Lengths (Å) and Angles (deg) for **8**

Zn(1)–O(1)	1.915(5)	O(2)–C(25)	1.345(8)
Zn(1)–P(1)	2.542(3)	O(1)–O(2)	1.923(5)
O(1)–C(7)	1.348(8)	Zn(1)–P(2)	2.588(3)
O(1)–Zn(1)–O(2)	108.8(2)	O(1)–Zn(1)–P(1)	102.1(2)
O(2)–Zn(1)–P(1)	120.3(2)	O(1)–Zn(1)–P(2)	116.8(2)
O(2)–Zn(1)–P(2)	102.7(2)	P(1)–Zn(1)–P(2)	107.01(9)
C(7)–O(1)–Zn(1)	137.3(4)	C(25)–O(2)–Zn(1)	130.1(4)

ability of PMe_3 vs tetrahydrofuran. First, the average Zn–O bond length of 1.919(5) Å is somewhat longer than that found in the THF-substituted derivative (1.876(5) Å).² More significantly, the O–Zn–O bond angle of 108.8(2)° in **8** is considerably less obtuse than the analogous angle in the THF adduct (142.9(2)°). Indeed, this value is more in accord with those observed in the trigonal planar monophosphine derivatives **1** (111.7(2)°) and **2** (103.2(2)°). The O–Zn–P bond angles varied widely from 102.11(16)° for $\angle\text{O}_1\text{–Zn–P}_1$ to 120.27(15)° for $\angle\text{O}_2\text{–Zn–P}_1$. Clearly, the THF derivative assumed a geometry that maximized the separation between the pendant *tert*-butyl groups, whereas **8**, by virtue of its larger and more donating PMe_3 ligands, conforms to a more symmetrical coordination sphere. At an average of 2.564(3) Å, the Zn–P bond lengths are significantly longer than the analogous bonds in **1** and **2** and longer than the Zn–P distance of 2.413(4) Å found in the $\text{Zn}(\text{S}-2,4,6\text{-Bu}_3\text{C}_6\text{H}_2)_2 \cdot \text{PMe}_3$ adduct. This is as expected on going from three-coordinate zinc to four-coordinate zinc.

Solution NMR Studies. We have previously described some preliminary ^{31}P NMR solution studies of phosphine binding studies to monomeric zinc(II) bisphenoxide complexes containing PPh_2Me (**1**) and PCy_3 (**2**) as donor ligands.²⁰ In both derivatives, the phosphines were completely bound to the zinc center in solution at ambient temperature and the exchange with the corresponding free phosphine was slow. That is, ^{31}P NMR measurements on pure samples of complexes **1** and **2** showed the shifted phosphorus resonances from that of the free phosphine to be temperature-independent over the range 25 to –90 °C in deuterated toluene. Moreover, addition of a second equivalent of the corresponding phosphine produced no discernible changes in the line shape or position of the ^{31}P resonances of these complexes. Hence, it is safe to conclude that there is no further binding of these phosphines to zinc nor are the phosphine ligands participating in a rapid self-exchange process. On the basis of chemical shift differences, the self-exchange lifetimes of free/bound phosphine must be considerably longer than 1.6 and 5.9×10^{-3} s for complexes **1** and **2**, respectively.

As a continuation of this work, we have compiled ^{31}P NMR data for a small library of different phosphine–phenoxide

Table 3. ^{31}P NMR Data of $\text{Zn}(\text{O}-2,6\text{-R}_2\text{C}_6\text{H}_3)_2 \cdot \text{Phosphine}$ Complexes in C_6D_6

complex	R substituents (positions)	phosphine	chemical shift, δ (ppm)	peak position of free ligand (ppm)
1	<i>t</i> -butyl	Ph_2PMe	–19.9 ^a	–26.6
2	<i>t</i> -butyl	PCy_3	7.74	10.1
3	<i>t</i> -butyl	PMe_3	–47.4	–62.3
4	<i>t</i> -butyl	PEt_3	–14.0	–19.5
5	<i>t</i> -butyl	PBu_3	–21.0	–31.5
6	<i>t</i> -butyl	$\text{Cy}_2\text{PCH}_2\text{PCy}_2$	–3.77	–10.9
7	<i>t</i> -butyl	Me_2PPh	–35.8	–45.9
9	phenyl	Ph_2PMe	0.29 ^a	–26.6
10	phenyl	PCy_3	12.2	10.1
11	phenyl	PMe_3	–48.8	–62.3
12	phenyl	PEt_3	–12.1(b)	–19.5
13	phenyl	PBu_3	–18.6(b) ^b	–31.5
15	methyl (2,4,6)	PBu_3	–21.0	–31.5

^a Measured in CD_2Cl_2 . ^b Measured in C_7D_8 .

complexes. The phosphorus chemical shift data for complexes **1–7**, **9–13**, and **15**, acquired in C_6D_6 or CD_2Cl_2 at ambient temperature, are collected in Table 3. From a cursory examination of Table 3 it is evident that the phosphines, which were found to significantly bind to zinc, were all good σ donors with cone angles less than 170°. For example, triphenylphosphine was not shown to afford an adduct with either of the zinc bisphenoxides examined herein. This prerequisite is apparently rather general for zinc derivatives, although numerous examples of cadmium complexes containing the less basic triphenylphosphine ligand are documented in the literature.^{24–26} At the same time, the phosphine cannot be too sterically demanding; for example, PBu_3 , which has a cone angle of 180°, did not coordinate to the zinc bisphenoxides. The ^{31}P chemical shifts for the bound phosphine were observed downfield of their respective positions as free ligands, with the exception of the upfield shift noted in complex **2**. Although in some of the bis-(diphenyl phenoxide) derivatives the ^{31}P NMR signals are broad (e.g., species **12** and **13**), variable temperature measurements from 20 to –80 °C in toluene-*d*₈ showed no indication of phosphine exchange.

Because the PMe_3 ligand is unique among the phosphines investigated in its reactivity toward the bis(phenoxide)zinc derivatives, affording both mono- and diphosphine adducts, it was of particular interest to examine the FT ^{31}P NMR spectra of this system. The ^{31}P spectrum of $\text{Zn}(\text{O}-2,6\text{-Bu}_2\text{C}_6\text{H}_3)_2$ in the presence of 1 equiv of PMe_3 at ambient temperature displays one resonance in toluene that undergoes a slight downfield shift as the temperature is lowered to –80 °C. In contrast, when 2.1 equiv of PMe_3 was added to $\text{Zn}(\text{O}-2,6\text{-Bu}_2\text{C}_6\text{H}_3)_2$, a single, fairly sharp ^{31}P signal appears at –55.5 ppm that is nearly equidistant from the bound and free positions at –47.4 and –62.3 ppm, respectively (Figure 5). As the temperature is lowered to 0 °C, the ^{31}P signal begins to migrate downfield. The signal continues to shift downfield and broaden further as the temperature is lowered to –60 °C where coalescence is approached. Below –60 °C, a second small signal surfaces at –62 ppm corresponding to that of the free phosphine. The peaks continue to narrow until, at –90 °C, two sharp peaks are observed at –48.9 and –62.3 ppm. The latter ^{31}P resonance is due to the slight excess of 2 equiv of PMe_3 used in the experiment. Hence, this behavior is readily understood in terms of the rapid equilibrium defined by eq 3, with the mono- PMe_3

(24) Cameron, A. F. *J. Chem. Soc. A* **1971**, 1286.

(25) Dakternieks, D. *Aust. J. Chem.* **1982**, 35, 469.

(26) Goel, R. G.; Jha, N. K. *Can. J. Chem.* **1981**, 59, 3267.

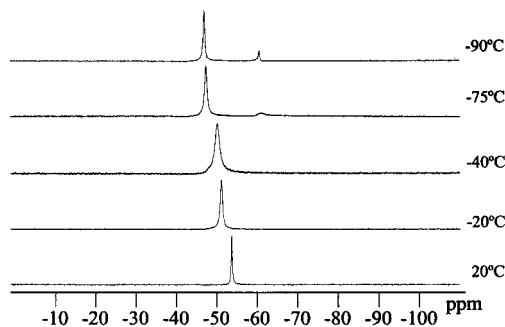
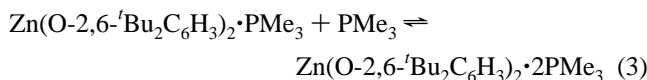


Figure 5. Temperature-dependent ^{31}P NMR spectra of $\text{Zn}(\text{O-2,6-}^t\text{Bu}_2\text{C}_6\text{H}_3)_2$ in the presence of 2.1 equiv of PMe_3 .

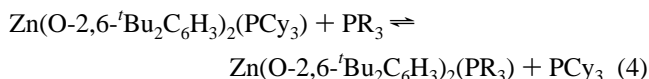
Table 4. Integrated Peak Areas of ^{31}P Signals for Bound and Free PEt_3 in Reaction 4 as a Function of Temperature

temp ($^\circ\text{C}$)	integration areas	
	bound PEt_3	free PEt_3
20	0.42	0.07
0	0.43	0.07
-20	0.44	0.06
-60	0.47	0.03
-80	0.47	0.03

adduct being the primary zinc-containing complex in solution at ambient temperature. As the temperature is lowered to -90°C , the equilibrium shifts to the right and the rate of exchange slows to reveal the $\text{Zn}(\text{O-2,6-}^t\text{Bu}_2\text{C}_6\text{H}_3)_2\cdot 2\text{PMe}_3$ derivative and free PMe_3 in the expected ratio of about 20:1 as dictated by the reaction's stoichiometry.



We have expanded these solution studies of bisphenoxide zinc derivatives in the presence of phosphines in order to determine their relative binding affinities. Rapid (NMR time scale) exchange, which occurs via an associative mechanism, has only been noted for the sterically unencumbering PMe_3 ligand. However, a much slower dissociative route is available to phosphine substitution in this zinc system, which occurs on the time scale of minutes even at low temperatures. These experiments were carried out starting from a pure sample of $\text{Zn}(\text{O-2,6-}^t\text{Bu}_2\text{C}_6\text{H}_3)_2(\text{PCy}_3)_2$, in the presence of an equimolar quantity of the appropriate phosphine in CD_2Cl_2 , and observing the equilibrium position of eq 4 as a function of temperature.



Complex **2** was utilized as the $\text{Zn}(\text{II})$ source in these studies because it is readily isolable in pure form, thus ensuring a 1:2 stoichiometry of zinc-to-phosphine ligands.

The equilibrium concentrations of the various species (free and zinc-bound phosphine ligands) were determined from the integrated areas of their ^{31}P resonances. In all instances, equilibrium was established within minutes, since no discernible changes were observed in the ^{31}P spectra of the mixtures obtained 15 and 45 min following addition of the phosphines. As might be anticipated, there was also not much change in the equilibrium position as a function of temperature as illustrated in Table 4 and Figure 6 for PR_3 equals PEt_3 . At 20°C the amount of bound triethylphosphine was determined to be 86% based on the integration of the peak intensities for the

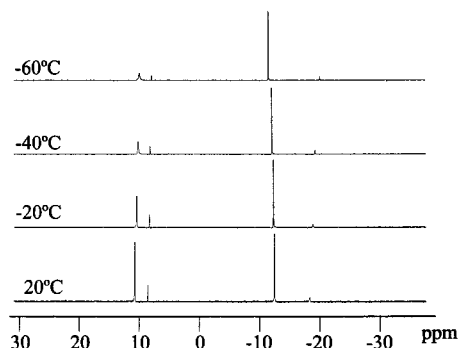


Figure 6. Temperature-dependent ^{31}P NMR spectra of $\text{Zn}(\text{O-2,6-}^t\text{Bu}_2\text{C}_6\text{H}_3)_2\cdot \text{PCy}_3$ plus 1 equiv of PEt_3 .

Table 5. K_{eq} for Phosphine Exchange Process Defined in Reaction 4^a

PR_3	K_{eq}	ΔG° (kcal/mol)
Ph_2PMe	9.9×10^{-2}	1.4
PEt_3	37.7	-2.2
PnBu_3	23.8	-1.9

^a Measured at ambient temperature.

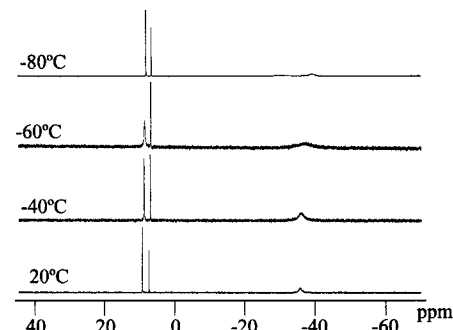


Figure 7. Temperature-dependent ^{31}P NMR spectra of $\text{Zn}(\text{O-2,6-}^t\text{Bu}_2\text{C}_6\text{H}_3)_2\cdot \text{PCy}_3$ plus 1 equiv of PPhMe_2 .

bound and free ligands at -13.0 and -19.0 ppm, respectively. A similar conclusion is reached from the ^{31}P NMR peak intensities of the bound and free PCy_3 ligand. Thus, the equilibrium expressed by eq 4 favors the smaller, slightly less basic ($\text{p}K_{\text{a}}$ of $\text{PEt}_3 = 8.69$ vs 9.70 for PCy_3)²⁷ phosphine.

Relative binding affinities of P^nBu_3 and PPh_2Me vs PCy_3 were determined in a similar manner. The equilibrium constants measured at ambient temperature for the process depicted in eq 4 are listed in Table 5, along with the respective standard free energy values. An analogous experiment was carried out employing the smaller ligand PPhMe_2 (cone angle 122°). However, in this case the zinc-bound PMe_2Ph species present in solution is in rapid equilibrium with free PMe_2Ph , analogous to the *associative* process observed for the other small phosphine, PMe_3 (vide supra). Figure 7 depicts the temperature-dependent ^{31}P spectra for this process, where we were unable to freeze out the exchange at -80°C . Nevertheless, from the ratio of the ^{31}P signals for free and bound PCy_3 it is possible to reason that approximately 75% of the zinc complex is involved in interactions with PPhMe_2 , which translates into 1.33 equiv of PPhMe_2 per zinc. Hence, zinc's binding affinity for PPhMe_2 is slightly greater than that for PCy_3 but less than that of P^nBu_3 or PEt_3 . Therefore, if we include the facts that 1 equiv of PMe_3 completely displaces PCy_3 from complex **2** and PPh_3 and P^nBu_3 are not able to displace PCy_3 from complex **2** to any

(27) Rahman, Md. M.; Liu, H.-Y.; Eriks, K.; Prock, A.; Giering, W. P. *Organometallics* **1989**, 8, 1.

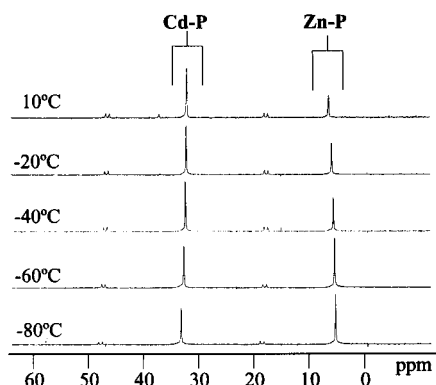
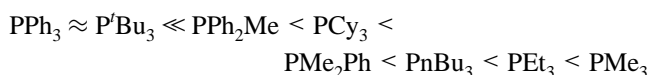


Figure 8. Temperature-dependent ^{31}P NMR spectra of equimolar mixture of $\text{Cd}(\text{O}-2,6\text{-}t\text{-Bu}_2\text{C}_6\text{H}_3)_2(\text{THF})_2$ and $\text{Zn}(\text{O}-2,6\text{-}t\text{-Bu}_2\text{C}_6\text{H}_3)_2(\text{THF})_2$ with 1 equiv of PCy_3 ($^{113}\text{Cd}-^{31}\text{P}$ and $^{111}\text{Cd}-^{31}\text{P}$ coupling noted).

measurable extent, the order of phosphine binding affinities to the sterically crowded zinc center in $\text{Zn}(\text{O}-2,6\text{-}t\text{-Bu}_2\text{C}_6\text{H}_3)_2$ is



In complementary undertakings we have been carrying out comparative structural and reactivity studies of analogous cadmium bis(phenoxide) derivatives to those presented herein involving zinc.^{28,29} These investigations have established that, primarily because of its larger size, the chemistry of cadmium is much more diverse when compared to that of zinc. For example, whereas $\text{Zn}(\text{O}-2,6\text{-}t\text{-Bu}_2\text{C}_6\text{H}_3)_2(\text{THF})_2$ is a distorted tetrahedral structure, its cadmium analogue is square-planar.^{15,30} Additionally, the cadmium phenoxide derivative binds three molecules of pyridine, whereas its zinc analogue binds two. In studies directly related to those reported herein, we have shown by ^{113}Cd NMR that $\text{Cd}(\text{O}-2,6\text{-}t\text{-Bu}_2\text{C}_6\text{H}_3)_2$ forms only a mono-phosphine adduct with the very large PCy_3 ligand.³¹ On the other hand, the smaller trialkylphosphines such as PR_3 ($\text{R} = \text{Me}, \text{Et}, n\text{-Bu}$) readily form diadducts. Hence, this system should allow us to demonstrate in a competitive experiment whether there is any kinetic or thermodynamic preference of PCy_3 for similar Zn/Cd sites.

To this end, an equimolar mixture of $\text{Cd}(\text{O}-2,6\text{-}t\text{-Bu}_2\text{C}_6\text{H}_3)_2(\text{THF})_2$ and $\text{Zn}(\text{O}-2,6\text{-}t\text{-Bu}_2\text{C}_6\text{H}_3)_2(\text{THF})_2$ in CD_2Cl_2 was added to a solution containing 1 equiv of PCy_3 at -78°C . The reaction's progress was monitored by ^{31}P NMR spectroscopy, with data collected incrementally over the temperature range -80° to 10°C as depicted in Figure 8. The initially observed cadmium to zinc-bound phosphine ratio is quite close to a statistical distribution, thus indicating little kinetic preference of PCy_3 for cadmium vs zinc. Changes in the product distribution as the temperature of the solution was increased are summarized in Figure 9. In the region between -80 and -60°C , where phosphine exchange is expected to be slow, the quantity of cadmium-bound phosphine vs zinc-bound phosphine was unchanged. However, when the mixture was warmed to -40°C , a significant increase in the concentration of the cadmium phosphine adduct, with a concomitant decrease in

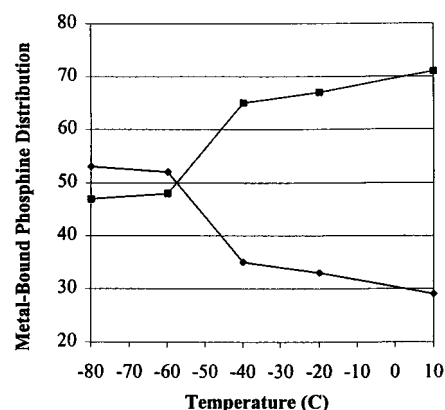


Figure 9. Plot of changes in $[\text{Cd-P}]/[\text{Zn-P}]$ distribution obtained from Figure 8 as the temperature is increased from -80 to $+10^\circ\text{C}$: (●) zinc-bound phosphine; (■) cadmium-bound phosphine.

Table 6. Zinc Bis(phenoxide)phosphine Catalyzed Copolymerization of CHO/CO_2 at 80°C and 800 psi CO_2 Pressure^a

aryl substituents (positions)	phosphine	% carbonate	% conversion ^b	turnovers ^c (g/g of Zn)
$t\text{-Bu}(2,6)$	PCy_3	92	36	806
$t\text{-Bu}(2,6)$	PCy_3^d	95	32	699
$t\text{-Bu}(2,4,6)$	PCy_3	98	39	852
$t\text{-Bu}(2,6)$	PPh_2Me	93	11	240

^a Reactions were carried out for about 62 h. ^b Calculated via integration of the ^1H NMR peak intensities for the bulk mixture.

^c Catalyst quantities used contained 0.013 g of Zn. ^d Reaction performed in the presence of additional 2 equiv of PCy_3 .

its zinc analogue, was observed. This change continued until $[\text{Cd-P}]/[\text{Zn-P}]$ was about 2.5 at 10°C with no significant changes occurring beyond this point. Hence, as might have been anticipated, there is a thermodynamic preference for phosphine cadmium binding vs phosphine zinc binding, albeit small. Consistent with the above interpretation, when the temperature of the thermodynamically established equilibrium mixture was lowered, no notable change in the complex distribution was observed.

Copolymerization of Cyclohexene Oxide (CHO) and Carbon Dioxide. In this section we examine the effect of addition donor ligands at the zinc center of zinc bis(phenoxides) on their efficacy as catalysts for the copolymerization of CHO/CO_2 to poly(cyclohexene carbonate). On the basis of the solution behavior of the various zinc bis(phenoxide) phosphine adducts described above, it is clear that the phosphine ligands, in the presence of weak alternative ligands such as CO_2 or epoxides, remain bound to the metal center under the conditions of the copolymerization reaction (eq 1). To quantitatively assess the consequence of phosphine ligands on reaction 1 catalyzed by bis($\text{O}-2,6\text{-}t\text{-Bu}_2\text{C}_6\text{H}_3$) $_2\text{Zn}$, we have employed pure samples of complexes **1** and **2** as catalysts. A summary of our observations is listed in Table 6.

Poly(alkylene)carbonate production in the absence of concurrent polyether formation is a desirable feature of good copolymerization catalysts. In other instances it is beneficial to be able to control the CO_2 content of the copolymer. Hence, the 2,6-di-*tert*-butylphenoxide and 2,4,6-tri-*tert*-butylphenoxide derivatives of zinc were utilized in these studies because we have previously shown these to produce the largest percentages of polyether linkages (greatest values of m in eq 1).^{1,2} Concomitantly, these zinc complexes are good catalysts for the homopolymerization of CHO to poly(cyclohexene oxide). It is immediately evident from the polymer runs in Table 6 that in the presence of PCy_3 , a strongly binding phosphine to zinc, these

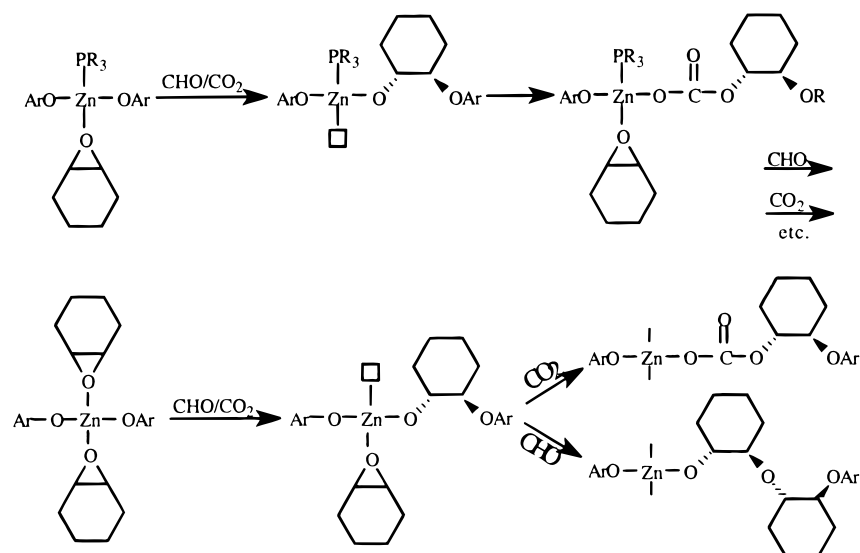
(28) Darensbourg, D. J.; Niezgoda, S. A.; Reibenspies, J. H.; Draper, J. D. *Inorg. Chem.* **1997**, 36, 5686.

(29) Darensbourg, D. J.; Niezgoda, S. A.; Draper, J. D.; Reibenspies, J. H. *J. Am. Chem. Soc.* **1998**, 120, 4690.

(30) Goel, S. C.; Chiang, M. Y.; Buhro, W. E. *J. Am. Chem. Soc.* **1990**, 112, 6724.

(31) Darensbourg, D. J.; Rainey, P.; Larkins, D. L.; Reibenspies, J. *Inorg. Chem.* **2000**, 39, 473.

Scheme 1



catalysts afford very high percentages of 1:1 copolymers. This is dramatically illustrated for the 2,4,6-*tert*-butylphenoxide derivative (entry 3 in Table 6), which in the absence of PCy_3 homopolymerizes cyclohexene oxide at ambient temperature. Indeed, to bring about copolymer production with this catalyst (<50% polycarbonate linkages), it was necessary to physically isolate the catalyst from the CHO prior to pressurizing the reactor with CO_2 , a procedure unnecessary in the presence of PCy_3 . At the same time the yield of copolymer (or activity of the catalyst) was not greatly affected by the presence of even 3 equiv of PCy_3 (entry 2). On the other hand, there is some reduction in copolymer yield in the presence of the less basic phosphine PPh_2Me . A similar, albeit less impressive, behavior was noted when PPh_3 was added to a triethylaluminum catalyst in an early report.³² Hence, it appears that only one metal binding site is required for copolymerization (recall that CO_2 insertion does not necessitate prior metal coordination),³³ but two binding sites are needed for consecutive epoxide insertions to be competitive with the very rapid CO_2 insertion process. This is summarized in Scheme 1. This interpretation is consistent with the observation that PMe_3 , which is capable of forming a bis(phosphine) adduct with zinc, completely inhibits catalysis. Recent results of Coates and co-workers⁵ further confirm this conclusion; that is, in this latter study, by use of a diimine zinc catalyst containing a methoxide or acetate ligand for initiation, no polyether formation was observed. Similarly, the soluble

dimeric species $\text{Zn}_2(\text{O}-2,6-\text{F}_2\text{C}_6\text{H}_3)_4 \cdot 2\text{THF}$, which has only one epoxide binding site, effectively catalyzes the copolymerization of CHO and CO_2 without formation of polyether linkages.³⁴ Correlatively, the insoluble zinc catalyst systems derived from the reaction of zinc oxide and dicarboxylic acids, which afford significant quantities of polyether linkages, must operate via a zinc center with two vacant sites for substrate binding.^{35,36} An additional consideration is that the binding of the weakly basic epoxide ligand to the zinc center may be reduced in the presence of electron-donating phosphine ligands; nevertheless, there is not a significant decrease in the rate of copolymerization in the presence of PCy_3 . This is amply demonstrated in the observation that the reactivity of $\text{Zn}(\text{O}-2,4,6-\text{tBu}_3\text{C}_6\text{H}_2)_2$ as a homopolymerization catalyst for CHO is greatly inhibited in the presence of PCy_3 .

Acknowledgment. The financial support of this research by the National Science Foundation (Grant CHE96-15866) and the Robert A. Welch Foundation is greatly appreciated.

Supporting Information Available: An X-ray crystallographic file in CIF format for the structure determination of complex **8**. This material is available free of charge via the Internet at <http://pubs.acs.org>. IC990594A

(32) Koinuma, H.; Hirai. *Makromol. Chem.* **1977**, 178, 1283.

(33) Darensbourg, D. J.; Mueller, B. L.; Bischoff, C. J.; Chojnacki, S. S.; Reibenspies, J. H. *Inorg. Chem.* **1991**, 30, 2418.

(34) Darensbourg, D. J.; Wildeson, J. R. Unpublished observations.

(35) Soga, K.; Imai, E.; Hattori, I. *Polym. J.* **1981**, 13, 407.

(36) (a) Rokicki, A. (Air Products and Chemicals, Inc. and Acro Chemical Co.) U.S. Patent 4,943,677, 1990. (b) Motika, S. (Air Products and Chemicals, Inc., Acro Chemical Co., and Mitsui Petrochemical Industries Ltd.) U.S. Patent 5,026,676, 1991.